Research Article | Vol. 25, No. 21 | 16 Oct 2017 | OPTICS EXPRESS 25960
Optics EXPRESS

Manipulating refractive index, homogeneity and spectroscopy of Yb^{3+}-doped silica-core glass towards high-power large mode area photonic crystal fiber lasers

FAN WANG,[1,2] LILI HU,[1] WENBIN XU,[1,2] MENG WANG,[1] SUYA FENG,[1] JINJUN REN,[1] LEI ZHANG,[1] DANPING CHEN,[1] NADÈGE OLLIER,[3] GUOJUN GAO,[4,5] CHUNLEI YU,[1,6] AND SHIKAI WANG[1,*]

[1]*Key Laboratory of Materials for High Power Laser, Shanghai Institute of Optics and Fine Mechanics, Chinese Academy of Sciences, Shanghai 201800, China*
[2]*University of Chinese Academy of Sciences, Beijing 100049, China*
[3]*Laboratoire des Solides Irradiés, UMR 7642, CEA–CNRS–Ecole Polytechnique, 91128 Palaiseau, France*
[4]*Institute of Microstructure Technology, Karlsruhe Institute of Technology (KIT), Eggenstein-Leopoldshafen 76344, Germany*
[5]*guojun.gao@kit.edu*
[6]*sdycllcy@163.com*
**woshiwsk@163.com*

Abstract: Output power scaling of single mode large mode area (LMA) photonic crystal fiber (PCF) amplifiers urgently requires the low refractive index of Yb^{3+}-doped silica glasses whilst maintaining high optical homogeneity. In this paper, we report on a promising alternative $Yb^{3+}/Al^{3+}/F^{-}/P^{5+}$-co-doped silica core-glass (YAFP), which is prepared by modified sol-gel method developed by our group and highly suitable for fabricating high power LMA PCF amplifiers. By controlling the doping combinations of $Al^{3+}/F^{-}/P^{5+}$ in Yb^{3+}-doped silica glass,it not only ensures low refractive index (RI) but also maintains the excellent optical homogeneity and spectroscopic properties of Yb^{3+}. The spectroscopic properties of Yb^{3+} ions have not deteriorated by the co-doping of F^{-} and P^{5+} in YAFP glass compared with that of Yb^{3+}/Al^{3+} co-doped silica glass. A large-size (⌀5 mm × 90 mm) YAFP silica-core glass rod with low average RI difference of 2.6×10^{-4} (with respect to pure silica glass), and low radial and axial RI fluctuations of $\sim 2 \times 10^{-4}$, was prepared. A LMA PCF with 50 μm core diameter was obtained by stack-capillary-draw techniques using YAFP core glass. Its core NA is 0.027. An average amplified power of 97 W peaking at 1030 nm and light-light efficiency of 54% are achieved from a 6.5 m long PCF in the pulse amplification laser experiment. Meanwhile, quasi-single-mode transmission is obtained with laser beam quality factor M^2 of 1.4.

OCIS codes: (160.2290) Fiber materials; (160.4760) Optical properties; (160.5690) Rare-earth-doped materials; (160.6060) Solgel; (160.6030) Silica.

References and links

1. R. Paschotta, J. Nilsson, A. C. Tropper, and D. C. Hanna, "Ytterbium-doped fibre amplifiers," IEEE J. Quantum Electron. **33**, 1049–1056 (1997).
2. J. Limpert, T. Schreiber, S. Nolte, H. Zellmer, T. Tunnermann, R. Iliew, F. Lederer, J. Broeng, G. Vienne, A. Petersson, and C. Jakobsen, "High-power air-clad large-mode-area photonic crystal fiber laser," Opt. Express **11**(7), 818–823 (2003).
3. Y. Qiao, N. Da, D. Chen, Q. Zhou, J. Qiu, and T. Akai, "Spectroscopic properties of neodymium doped high silica glass and aluminum codoping effects on the enhancement of fluorescence emission," Appl. Phys. B **87**, 717–722 (2007).

#302148 https://doi.org/10.1364/OE.25.025960
Journal © 2017 Received 11 Jul 2017; revised 28 Sep 2017; accepted 29 Sep 2017; published 10 Oct 2017

Optics EXPRESS

4. E. Coscelli, F. Poli, T. T. Alkeskjold, M. M. Jørgensen, L. Leick, J. Broeng, A. Cucinotta, and S. Selleri, "Thermal Effects on the Single-Mode Regime of Distributed Modal Filtering Rod Fiber," J. Lightwave Technol. **30**, 3494–3499 (2012).
5. C. Jauregui, J. Limpert, and A. Tünnermann, "High-power fibre lasers," Nat. Photonics **7**, 861–867 (2013).
6. W. He, M. Leich, S. Grimm, J. Kobelke, Y. Zhu, H. Bartelt, and M. Jäger, "Very large mode area ytterbium fiber amplifier with aluminum-doped pump cladding made by powder sinter technology," Laser Phys. Lett. **12**, 015103 (2014).
7. A. Galvanauskas, "High Power Fiber lasers," Opt. Photonics News **15**, 42–47 (2004).
8. Z. Wang, Q. Li, Z. Wang, F. Zou, Y. Bai, S. Feng, and J. Zhou, "255 W picosecond MOPA laser based on self-made Yb-doped very-large-mode-area photonic crystal fiber," Chin. Opt. Lett. **14**, 54–57 (2016).
9. J. Limpert, A. Liem, M. Reich, T. Schreiber, S. Nolte, H. Zellmer, A. Tünnermann, J. Broeng, A. Petersson, and C. Jakobsen, "Low-nonlinearity single-transverse-mode ytterbium-doped photonic crystal fiber amplifier," Opt. Express **12**(7), 1313–1319 (2004).
10. D. Liang, Advanced Optical Fibers for High Power Fiber Lasers in *Advances in Optical Fiber Technology: Fundamental Optical Phenomena and Applications*, M. Yasin, ed. (InTech, 2015).
11. V. Petit, R. P. Tumminelli, J. D. Minelly, and V. Khitrov, "Extremely low NA Yb doped preforms (<0.03) fabricated by MCVD," Proc. SPIE **9728**, 97282R (2016).
12. M. Likhachev, S. Aleshkina, A. Shubin, M. Bubnov, E. Dianov, D. Lipatov, and A. Guryanov, "Large-Mode-Area Highly Yb-doped Photodarkening-Free Al_2O_3-P_2O_5-SiO_2-Based Fiber," in Proceedings of CLEO/Europe and EQEC 2011 Conference Digest, OSA Technical Digest (CD) (Optical Society of America, 2011), paper CJ_P24.
13. M. Y. Koptev, E. A. Anashkina, K. K. Bobkov, M. E. Likhachev, A. E. Levchenko, S. S. Aleshkina, S. L. Semjonov, A. N. Denisov, M. M. Bubnov, D. S. Lipatov, A. Y. Laptev, A. N. Gur'yanov, A. V. Andrianov, S. V. Muravyev, and A. V. Kim, "Fibre amplifier based on an ytterbium-doped active tapered fibre for the generation of megawatt peak power ultrashort optical pulses," Quantum Electron. **45**, 443–450 (2015).
14. K. K. Bobkov, M. Y. Koptev, A. E. Levchenko, S. S. Aleshkina, S. L. Semenov, A. N. Denisov, M. M. Bubnov, D. S. Lipatov, A. Y. Laptev, A. N. Guryanov, E. A. Anashkina, S. V. Muravyev, A. V. Andrianov, A. V. Kim, and M. E. Likhachev, "MW peak power diffraction limited monolithic Yb-doped tapered fiber amplifier," Proc. SPIE **10083**, 1008309 (2017).
15. W. Xu, C. Yu, S. Wang, F. Lou, S. Feng, M. Wang, Q. Zhou, D. Chen, L. Hu, and M. Guzik, "Effects of F^- on the optical and spectroscopic properties of Yb^{3+}/Al^{3+}-co-doped silica glass," Opt. Mater. **42**, 245–250 (2015).
16. J. J. Koponen, L. C. Petit, T. Kokki, V. Aallos, J. Paul, and H. Ihalainen, "Progress in direct nanoparticle deposition for the development of the next generation fiber lasers," Opt. Eng. **50**, 1605 (2011).
17. K. Schuster, S. Unger, C. Aichele, F. Lindner, S. Grimm, D. Litzkendorf, J. Kobelke, J. Bierlich, K. Wondraczek, and H. Bartelt, "Material and technology trends in fiber optics," Adv. Opt. Technol. **3**, 447–468 (2014).
18. U. Pedrazza, V. Romano, and W. Lüthy, "Yb^{3+}:Al^{3+}:sol-gel silica glass fiber laser," Opt. Mater. **29**, 905–907 (2007).
19. K. Schuster, S. Grimm, A. Kalide, J. Dellith, M. Leich, A. Schwuchow, A. Langner, G. Schötz, and H. Bartelt, "Evolution of fluorine doping following the REPUSIL process for the adjustment of optical properties of silica materials," Opt. Mater. Express **5**, 887–897 (2015).
20. H. El Hamzaoui, G. Bouwmans, A. Cassez, L. Bigot, B. Capoen, M. Bouazaoui, O. Vanvincq, and M. Douay, "F/Yb-codoped sol-gel silica glasses: toward tailoring the refractive index for the achievement of high-power fiber lasers," Opt. Lett. **42**(7), 1408–1411 (2017).
21. W. Xu, Z. Lin, M. Wang, S. Feng, L. Zhang, Q. Zhou, D. Chen, L. Zhang, S. Wang, C. Yu, and L. Hu, "50 μm core diameter $Yb^{3+}Al^{3+}/F^-$ codoped silica fiber with M^2<1.1 beam quality," Opt. Lett. **41**(3), 504–507 (2016).
22. M. E. Likhachev, M. M. Bubnov, K. V. Zotov, D. S. Lipatov, M. V. Yashkov, and A. N. Guryanov, "Effect of the $AlPO_4$ join on the pump-to-signal conversion efficiency in heavily Er-doped fibers," Opt. Lett. **34**(21), 3355–3357 (2009).
23. S. Wang, F. Lou, C. Yu, Q. Zhou, M. Wang, S. Feng, D. Chen, L. Hu, W. Chen, and M. Guzik, "Influence of Al^{3+} and P^{5+} ion contents on the valence state of Yb^{3+} ions and the dispersion effect of Al^{3+} and P^{5+} ions on Yb^{3+} ions in silica glass," J. Mater. Chem. C Mater. Opt. Electron. Devices **2**, 4406–4414 (2014).
24. D. J. Digiovanni, J. B. Macchesney, and T. Y. Kometani, "Structure and properties of silica containing aluminum and phosphorus near the $AlPO_4$ join," J. Non-Cryst. Solids **113**, 58–64 (1989).
25. A. Morana, S. Girard, M. Cannas, E. Marin, C. Marcandella, P. Paillet, J. Périsse, J. R. Macé, R. Boscaino, and B. Nacir, "Influence of neutron and gamma-ray irradiations on rad-hard optical fiber," Opt. Mater. Express **5**, 898–911 (2015).
26. S. Wang, W. Xu, F. Wang, F. Lou, L. Zhang, Q. Zhou, D. Chen, S. Feng, M. Wang, C. Yu, and L. Hu, "Yb^{3+}-doped silica glass rod with high optical quality and low optical attenuation prepared by modified sol-gel technology for large mode area fiber," Opt. Mater. Express **7**, 2012 (2017).
27. W. Xu, M. Wang, S. Feng, and L. Zhang, "Fabrication and Laser Amplification Behavior of Yb^{3+}/Al^{3+} Co-Doped Photonic Crystal Fiber," IEEE Photonics Technol. Lett. **28**, 391–393 (2016).
28. D. J. DiGiovanni, J. B. MacChesney, and T. Y. Kometani, "Structure and properties of silica containing aluminum and phosphorus near the AlPO4 join," J. Non-Cryst. Solids **113**, 58–64 (1989).

Optics EXPRESS

29. B. Yang, X. Liu, X. Wang, J. Zhang, L. Hu, and L. Zhang, "Compositional dependence of room-temperature Stark splitting of Yb^{3+} in several popular glass systems," Opt. Lett. **39**(7), 1772–1774 (2014).
30. W. Xu, C. Yu, S. Wang, F. Lou, S. Feng, M. Wang, Q. Zhou, D. Chen, L. Hu, M. Guzik, and G. Boulon, "Effects of F^- on the optical and spectroscopic properties of Yb^{3+}/Al^{3+}-co-doped silica glass," Opt. Mater. **42**, 245–250 (2015).
31. W. Xu, J. Ren, C. Shao, X. Wang, M. Wang, L. Zhang, D. Chen, S. Wang, C. Yu, and L. Hu, "Effect of P^{5+} on spectroscopy and structure of $Yb^{3+}/Al^{3+}/P^{5+}$ co-doped silica glass," J. Lumin. **167**, 8–15 (2015).
32. G. Gao, M. Peng, and L. Wondraczek, "Temperature dependence and quantum efficiency of ultrabroad NIR photoluminescence from Ni^{2+} centers in nanocrystalline Ba-Al titanate glass ceramics," Opt. Lett. **37**(7), 1166–1168 (2012).
33. G. Gao, A. Winterstein-Beckmann, O. Surzhenko, C. Dubs, J. Dellith, M. A. Schmidt, and L. Wondraczek, "Faraday rotation and photoluminescence in heavily Tb^{3+}-doped GeO_2-B_2O_3-Al_2O_3-Ga_2O_3 glasses for fiber-integrated magneto-optics," Sci. Rep. **5**, 8942 (2015).
34. J. Kirchhof, S. Unger, A. Schwuchow, S. Grimm, and V. Reichel, "Materials for high-power fiber lasers," J. Non-Cryst. Solids **352**, 2399–2403 (2006).
35. J. Kirchhof, S. Unger, A. Schwuchow, S. Jetschke, V. Reichel, M. Leich, and A. Scheffel, "The influence of Yb ions on optical properties and power stability of ytterbium-doped laser fibers," Proc. SPIE **7598**, 75980B (2010).
36. S. Rydberg and M. Engholm, "Experimental evidence for the formation of divalent ytterbium in the photodarkening process of Yb-doped fiber lasers," Opt. Express **21**(6), 6681–6688 (2013).
37. K. K. Bobkov, "Charge-transfer state excitation as the main mechanism of the photodarkening process in ytterbium-doped aluminosilicate fibres," Quantum Electron. **44**, 1129–1135 (2014).

1. Introduction

Yb^{3+}-doped silica fibers have been the most important gain medium for high-power laser applications, owing to the small quantum defect of Yb^{3+} ions and the excellent mechanical strength of silica glass [1–3]. With the increase of laser output power, conventional double-clad fibers suffer from nonlinear effects and even damage of fiber end facets, which limit their maximum output power and degrade laser beam quality [4–6]. Large mode area (LMA) fibers can reduce laser power density and hence increase the thresholds of thermal damage and nonlinear effects during high-power pumping due to their large core diameter and effective mode area. Thus, Yb^{3+}-doped LMA fibers have been the subject of intense research during the past decade [7,8].

LMA fibers can effectively suppress nonlinear effects, but their laser beam quality is seriously deteriorated with increasing core diameter [9]. For an effective single-mode operation, many LMA fiber designs require the refractive indices of the fiber core and cladding to be nearly equal [10]. Therefore, the greatest challenge of fabricating LMA fibers is the preform preparation, requiring low RI and high doping homogeneity in the core glass. Nowadays, the commercial preparation technology-modified chemical vapor deposition (MCVD) combined with solution doping is difficult to realize large-size active core and ideal refractive index distribution directly. An alternative technology is using gas-phase doping in MCVD system, where large-size Yb^{3+}-doped silica core with high homogeneity has been achieved. Petit et al [11] have successfully prepared an $Yb^{3+}/Al^{3+}/F^-$-co-doped silica preform for double-clad fibers using a proprietary rare-earth vapor delivery system coupled to a standard MCVD lathe and achieved a low numerical aperture (NA) of 0.025 ± 0.005. M. E. Likhachev et al [12–14] developed an $Yb^{3+}/Al^{3+}/P^{5+}$-co-doped active tapered cladding fiber with a core diameter of 67 um and core flatness was good to get perfect Gaussian mode shape with $M^2 < 1.15$. For preparing LMA fiber using gas-phase doping technology, the RI difference between core and cladding should be further decreased. An effective method to decrease the RI of Yb^{3+} doped core glass is incorporation of F^-. Using this approach, the refractive index can be adjusted to be equal to or even lower than that of pure silica glass [15]. However, the direct incorporation of F^- during MCVD-based techniques is of limited use, since the high volatility of fluoride during preform collapsing. The key issue of LMA fiber doping with F^- is the accurate control of the refractive index and its fluctuation in radial and axial directions. Under these circumstances, other non-CVD fabrication technologies have been developed and reported, such as direct nanoparticle deposition (DND), reactive powder sintering of silica (REPUSIL), and sol-gel methods [16–18]. Heraeus Quarzglas has

Optics EXPRESS

made great progress in the preparation of $Yb^{3+}/Al^{3+}/F^{-}$-co-doped silica bulk glasses, with the F^{-}-doping-induced RI reduction being obvious, but the homogeneity is not good enough [19]. F^{-}/Yb^{3+}-co-doped sol-gel silica glasses have been reported recently and the Yb_2O_3-doping level of about 0.18 wt.% [20]. Our groups have been committed to the preparation of large Yb^{3+}-doped silica glass rod with low refractive index and high optical homogeneity by modified sol-gel method combined with high-temperature sintering. The so-gel process ensures that the raw materials is mixing in molecular level, which is vitally important to make uniform doped powder for sintering. In our previous study, we reported $Yb^{3+}/Al^{3+}/F^{-}$-co-doped glass and fiber [21]. However, the achieved radial refractive index fluctuation was still as high as 4×10^{-4}.

The co-doping of aluminum and phosphorus is well known to increase the solubility of rare earth ions in silica glass [22]. Moreover, the incorporation of P^{5+} into Yb^{3+}/Al^{3+}-co-doped silica glass can reduce the number of Yb^{2+} ions and reduce the refractive index due to the formation of $AlPO_4$ joint [23, 24]. F^{-} doping has a significant effect on photodarkening and radiation-induced darkening [19, 25]. To the best of our knowledge, few studies on $Yb^{3+}/Al^{3+}/F^{-}/P^{5+}$-co-doped silica glass used as an active core is reported due to the difficulty in preparing glass rod with low refractive index and high optical homogeneity. In this work, F^{-} and P^{5+} were simultaneously introduced into Al^{3+}/Yb^{3+}-doped silica glass to form an $Yb^{3+}/Al^{3+}/F^{-}/P^{5+}$-co-doped silica-core glass rod, and its optical homogeneity was improved by optimizing the doping components and sol-gel process parameters. Radial and axial refractive index fluctuations of $\sim 2 \times 10^{-4}$ were realized, and a small RI difference (2.6×10^{-4}) between the core glass and pure silica glass was achieved. To the best of our knowledge, our work presents the first-time report of a large-size (⌀5 mm × 90 mm) $Yb^{3+}/Al^{3+}/F^{-}/P^{5+}$-co-doped silica glass rod with high optical homogeneity and a low refractive index, fabricated by sol-gel method combined with high-temperature sintering. Using this core-glass rod, a LMA PCF with a core diameter of 50 μm was prepared.

2. Experimental

Silica glasses co-doped with Yb^{3+}/Al^{3+} (YA), $Yb^{3+}/Al^{3+}/F^{-}$ (YAF) and $Yb^{3+}/Al^{3+}/F^{-}/P^{5+}$ (YAFP) were prepared by modified sol-gel method. The detailed nominal compositions of glasses and sample preparation process are shown in Table 1 and Fig. 1, respectively. High purity tetraethoxysilane (TEOS, MOS, Kermel), $AlCl_3 \cdot 6H_2O$ (99.9995%, Alfa), $YbCl_3 \cdot 6H_2O$ (99.99%, Alfa), $(NH_4)_2SiF_6$ (99.999%, Alfa) and H_3PO_4 (85 wt%, Alfa) were used as precursors. Ethanol (MOS, Kermel) and deionized water were added to sustain the hydrolysis reaction. $AlCl_3 \cdot 6H_2O$, H_3PO_4, $YbCl_3 \cdot 6H_2O$, and TEOS were weighed to achieve the sample molar compositions. $(NH_4)_2SiF_6$ was introduced by a molar ratio of F^{-}/Si^{4+} in sol-gel process. All reagents were mixed and thoroughly stirred at 30 °C to form a homogeneous and transparent doped gel which was heated from 80 to 1100 °C to produce a dry powder and achieve almost complete decomposition of organic components. The obtained powder was melted at 1750 °C for 2.5 hours under vacuum to form glass. The glasses were cut and polished to 2-mm thick slices for spectroscopic measurements. The bulk glass can be further molded into a core-glass rod. The YAFP core glass rod with size of ⌀5 mm × 90 mm was prepared by the same method. Then, a LMA PCF was drawn by the stack-capillary-draw techniques at 2000 °C as described in our earlier publications [26].

The refractive index profiles of all samples were tested using a Photon Kinetics PK2600 instrument at 633 nm. The Al^{3+}, P^{5+}, and Yb^{3+} contents of glass samples were determined by inductively coupled plasma optical emission spectrometry (ICP-OES; radial-view Thermo iCAP 6300) after complete dissolution of the sample in aqueous HF. The F^{-} content was measured by electron probe microanalysis (EPMA, JXA8230), with the test error being less than 10%. A Heraeus Quarzglas quartz tube with a F^{-} doping concentration of 65000 ppm (mass fraction) was used as a reference. Absorption spectra were recorded in the range of 200–1200 nm using a Lambda 950 UV-VIS-NIR spectrophotometer. Emission spectra

Optics EXPRESS

(pumped with a Xe lamp at 896 nm) and decay curves of Yb^{3+} (pumped with a pulsed 975-nm diode laser) and emission spectra of Yb^{2+} (pumped with a Xe lamp at 330 nm) were measured on a high-resolution spectrofluorometer (Edinburgh Instruments, FLS 920). The homogeneity of Al^{3+}, P^{5+}, and F^- distributions in the glass rod was characterized by electron micro probe analyzer (EPMA) line scanning. The area distribution of Yb ions (30 μm × 30 μm) was characterized by EPMA elemental mapping.

Table 1. Nominal compositions of glass samples

Sample	Yb_2O_3 (mol.%)	Al_2O_3 (mol.%)	P_2O_5 (mol.%)	SiO_2 (mol.%)	F^-/Si^{4+} (mol.%)
YA	0.075	1	0	98.925	0
YAF	0.075	1	0	98.925	2.5
YAFP1	0.075	1	0.2	98.725	2.5
YAFP2	0.075	0.9	0.2	98.825	2.5

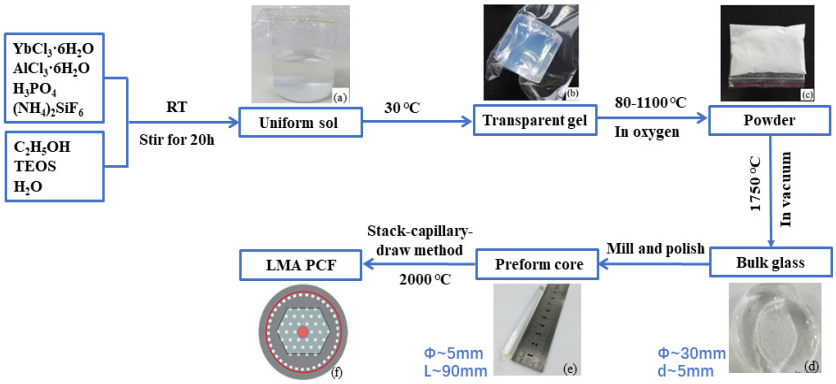

Fig. 1. The fabrication process of Yb^{3+}-doped silica-core glass rod and LMA PCF.

3. Results and discussion

3.1 Doping homogeneity of the core-glass rod

As mentioned in introduction, for an effective single-mode operation of LMA PCFs, the refractive index of core glass should be nearly equal to the cladding pure silica glass to ensure low numerical aperture (NA). For high-power fiber lasers, the doping of Yb^{3+} and Al^{3+} in silica core glass leads to the high refractive index of the silica-core glass. The co-doping of elements such as F^- and P^{5+} is the straightforward way to reduce the refractive index of silica core glass. But the co-doping of F^- and P^{5+} in YAFP glass could deteriorate the optical homogeneity of silica glass due to the volatizing effect during high temperature melting. In this study, we optimized our newly developed modified sol-gel method to decrease the refractive index of silica core glass by co-doping of F^-/P^{5+} in YAFP silica-core glass, whilst maintaining the good homogeneity and spectroscopic properties of Yb^{3+}.

The radial refractive index profiles of YA, YAF, YAFP1 and YAFP2 glass rods at 633 nm are shown in Fig. 2(a). It is noteworthy that the obvious fluctuation in the center (± 0.2 mm) is a numerical artifact probably caused by the fitting error [27]. Figure 2(b) shows the pictures of YA, YAF and YAFP1 glass rods. The refractive index difference Δn with respect to the pure un-doped silica glass is 19.2 ± 2 × 10^{-4}, 12.3 ± 3 × 10^{-4}, 8.4 ± 3 × 10^{-4} and 2.6 ± 2 × 10^{-4} for YA, YAF, YAFP1 and YAFP2 glasses, respectively. The corresponding core numerical aperture (NA) is calculated to be 0.075, 0.060, 0.049 and 0.027, respectively. The low NA value of YAFP2 glass is suitable for LMA PCF fiber fabrication. The co-doing of F^- and P^{5+} and decreasing the co-doping concentration of Al^{3+} in YA glass effectively decrease the refractive index of YA silica-core glass. In detail, the co-doping of light F^- in YAF glass reduces Δn from 19.2 ± 2 × 10^{-4} of YA glass to 12.3 ± 3 × 10^{-4}. The concentration of F^- in

Optics EXPRESS

glasses (which is measured by EPMA) is shown in Table 2. The content of F^- is much lower than theoretical value due to F^- volatilization during high-temperature sintering process. The further doping of P^{5+} in YAFP glass reduces Δn from $12.3 \pm 3 \times 10^{-4}$ of YAF glass to $8.4 \pm 3 \times 10^{-4}$, due to the formation of $AlPO_4$-like unit at the molar ratio of $P^{5+}/Al^{3+} < 1$ [28]. The standard deviation of the refractive index fluctuations of YA, YAF, YAFP1 and YAFP2 glasses is 2×10^{-4}, 3×10^{-4}, 3×10^{-4} and 2×10^{-4}, respectively. Refractive index fluctuations or variations of YAF and YAFP1 glass are slightly higher than that of YA glass due to the aforementioned volatilizing effect of F^- and P^{5+}, while YAFP2 glass is almost as good as that of YA glass.

Table 2. The Δn, corresponding core numerical apertures and tested F^- content in glass samples

Sample	Ä*n*	Core NA	F^- content (wt.%)
YA	19.2×10^{-4}	0.075	0
YAF	12.3×10^{-4}	0.060	0.32
YAFP1	8.4×10^{-4}	0.049	0.33
YAFP2	2.6×10^{-4}	0.027	0.35

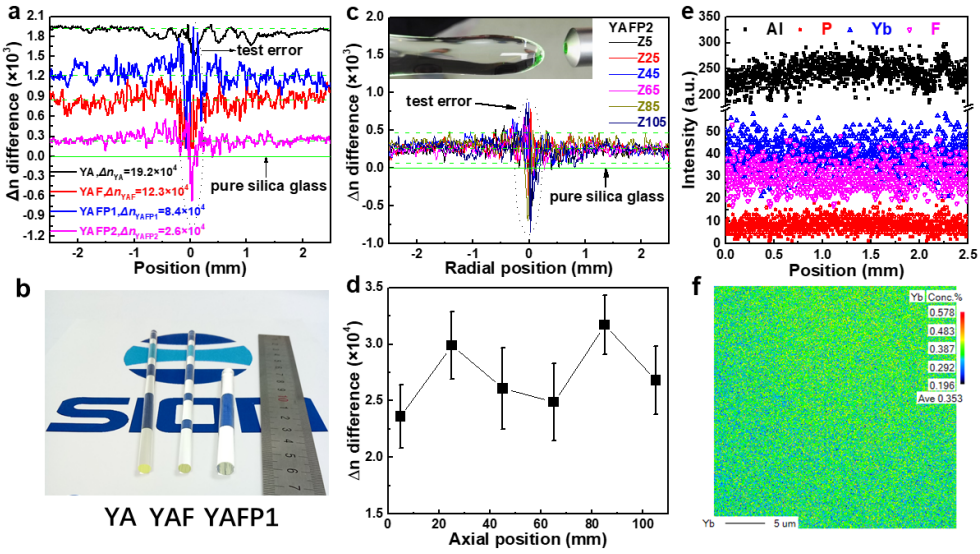

Fig. 2. (a) Radial RI profiles and (b) pictures of silica glass rods. (c) RI profile of YAFP2 glass rod at different axial positions with an image of the prepared glass illuminated by a green laser pointer (inset) and (d) Variation of RI difference along the length of glass rod. (e) EPMA radial line scan analysis of core-glass slices: Yb, Al, P, and F radial line distributions and (f) EPMA map (30 μm × 30 μm) of Yb distribution in core of PCF described herein.

YAFP2 glass not only has lower refractive index but also maintains the excellent optical homogeneity and spectroscopic properties of Yb^{3+}. Thus, it is a promising alternative core-glass for fabricating high-power LMA PCF amplifiers. The large-size high quality YAFP2 core-glass rod sized ⌀5 mm × 90 mm was prepared for LMA PCF fabrication. Figure 2(c) shows refractive index profile of YAFP2 glass-core rod at 633 nm. As shown in Figs. 2(c) and 2(d), the refractive index fluctuations in both radial and axial directions are $\sim 2 \times 10^{-4}$, which confirms the excellent optical homogeneity of YAFP2 core-glass rod. The average refractive index difference of $2.6 \pm 2 \times 10^{-4}$ of YAFP2 (with respect to the pure silica glass) is corresponding to a core NA of 0.027. It is suitable for fabricating the single-mode LMA PCF amplifier. As shown in the inset of Fig. 2(c), no bubbles and scattering points in YAFP2 glass was found, illuminated by a green laser (532 nm, < 50 mW). It is vitally important for controlling background attenuation of PCF.

Optics EXPRESS

The doping homogeneity of Yb, Al, P, and F is further confirmed by EPMA radial line scan analysis of the core-glass slice, as illustrated in Fig. 2(e). All elements show uniform distribution in YAFP2 glass rod. The EPMA mapping of Yb distribution in core of PCF in Fig. 2(f) confirms the high doping homogeneity of Yb ions.

3.2 Spectroscopic properties of $Yb^{3+}/Al^{3+}/F^{-}/P^{5+}$-co-doped glass

YAFP1 and YAFP2 glasses yield almost identical spectroscopic and structure properties in reflection of their highly similar chemical composition. In following, we only present the spectroscopic and structural results of YAFP1. Figure 3(a) shows absorption spectra of YA, YAF and YAFP1 glasses in NIR region. The characteristic absorption profile of Yb^{3+} covers a broad spectral region from 840 to 1000 nm. They are comprised of a sharp peak at ~975 nm and a broad shoulder at ~915 nm, ascribed to the transition from ground state (Yb^{3+}:$^2F_{7/2}$) to three Stark levels of the excited state (Yb^{3+}:$^2F_{5/2}$), as illustrated in Fig. 3(c). The peak position of the sharp peak keeps constant at ~975 nm with co-doping of F^- (YAF) or F^-/P^{5+} (YAFP1) in YA glasses. Whereas, the co-doping of F^- or F^-/P^{5+} in YA glasses leads to the slight red shift of the peak position of the broad shoulder from ~914 to 915 nm, which hints the mild modification of local environment around Yb^{3+} by co-doping of F^- or F^-/P^{5+} in YA glasses.

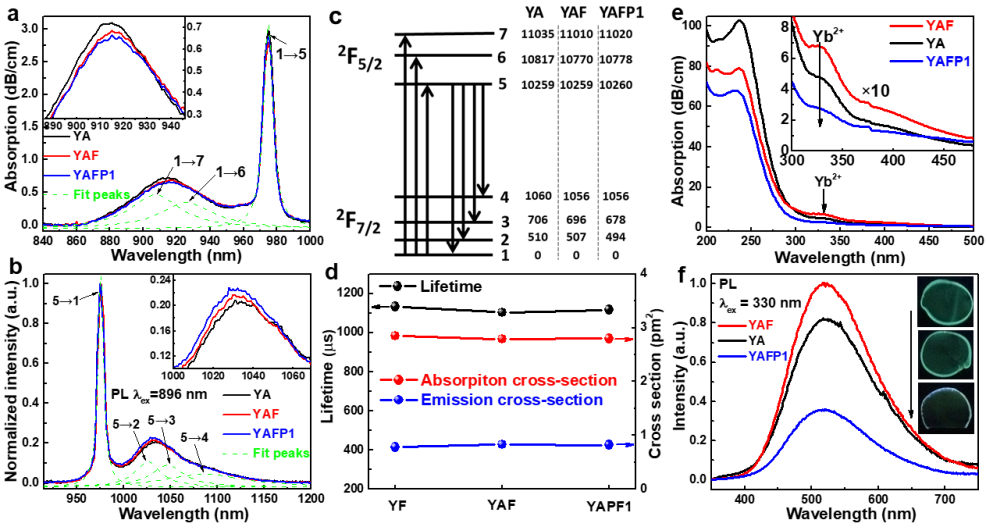

Fig. 3. (a) Absorption and (b) normalized emission spectra of Yb^{3+} for YA, YAF and YAFP1 glass samples. (c) Schematic manifolds energy diagram of Yb^{3+} ion derived from the Lorenz fitting of the absorption and emission spectrum of Yb^{3+}. (d) Absorption and emission cross-section and lifetime of glass samples. (e) Absorption and (f) fluorescence spectra of Yb^{2+} in YA, YAF and YAFP1 glass samples.

Figure 3(b) shows the emission spectra of YA, YAF and YAFP1 glasses. With irradiation with a Xe lamp at 896 nm, the typical emission profile of Yb^{3+} spans a broad spectral region from 940 to 1150 nm and is composed of a sharp peak at ~975 nm and three shoulders at ~1025, ~1045 and ~1090 nm. They are attributed to the transition from the excited state of Yb^{3+}:$^2F_{5/2}$ to four Stark levels of Yb^{3+}:$^2F_{7/2}$, as shown in Fig. 3(c). The emission peak position slightly shifts by co-doping of F^- (YAF) or F^-/P^{5+} (YAFP) in YA glasses, which proofs the mild modification of local environment around Yb^{3+} by co-doping of F^- or F^-/P^{5+} in YA glasses. For example, the peak position varies for YA (1031 nm), YAF (1030 nm) and YAFP1 (1028 nm) glasses. To have a more precise idea of the stark levels, we resolved each spectrum by the Lorentz analysis method and the maximum Stark splitting energies of $^2F_{7/2}$ and $^2F_{5/2}$ manifolds are listed in Fig. 3(c). It should be noted that there is no obvious Stark splitting difference of Yb^{3+} in glass matrix between low temperature and room temperature

Optics EXPRESS

[29], which is different from crystal materials. Therefore, the room-temperature absorption and emission spectra were used for the analysis of Stark levels splitting. Based on our early systematic study [30, 31], co-doping with F^- leads to the red shift of (1 → 6,7) absorption transitions and blue shift of (5 → 2,3,4) emission transitions. Co-doping with P^{5+} leads to the blue shifting of absorption transitions and emission transitions. In this work, the results are fully consistent with our former studies.

The absorption (σ_{abs}) and stimulated emission cross-sections (σ_{em}) of Yb^{3+} in YA, YAF and YAFP1 glasses are calculated according to the Beer-Lambert law and Füchtbauer-Landenburg (F-L) equations, respectively [32]. The σ_{abs} at 975 nm (absorption peak of Yb^{3+}) is calculated to be ~2.8×10^{-20} cm^2. The co-doping of F^- or F^-/P^{5+} in YA glasses maintains these values. The σ_{em} at 1030 nm (lasering peak position) is determined to be 0.78×10^{-20} cm^2. The co-doping of F^- or F^-/P^{5+} in YA glasses slightly increase the σ_{em} [Fig. 3(d) and Table 3]. The product of $\sigma_{em}*\tau$ is frequently used as optical gain parameter for fiber lasers, which is proportion to the amplification gain and inverse to laser oscillation threshold [33]. YA glass shows a large $\sigma_{em}*\tau$ value of 8.8×10^{-24} cm^2·s, which slightly increases with co–doping of F^- (YAF) or F^-/P^{5+} (YAFP1) in YA glasses. As summarized in Fig. 3(d) and Table 3, the decay lifetime ($\tau_{1/e}$, λ_{ex} = 975 nm) of Yb^{3+} emission at 1030 nm for YA, YAF and YAFP1 glasses almost keeps constant, ~1120 μs. The almost unchanged lifetime ($\tau_{1/e}$) and absorption (σ_{abs}), and slightly increased stimulated emission cross-section (σ_{em}) and optical gain parameter ($\sigma_{em}*\tau$) of Yb^{3+} evidences the co-doping by F^- (YAF) and F^-/P^{5+} (YAFP) maintains or even improves the excellent spectroscopic properties of Yb^{3+} in YA glass.

Table 3. Comparisons of fluorescence lifetimes (τ) at 1030 nm, absorption cross-sections at 975 nm (σ_{abs}), emission cross-sections at 1030 nm (σ_{em}), and optical gain parameter ($\sigma_{em}*\tau$) at 1030 nm in Yb^{3+} doped silica-core glass.

Sample	ô (is)	ó$_{abs}$ (pm^2)	ó$_{em}$ (pm^2)	ó$_{em}$*ô (cm^2·s)
YA	1132	2.85	0.78	8.8×10^{-24}
YAF	1103	2.79	0.83	9.2×10^{-24}
YAPF1	1117	2.80	0.82	9.2×10^{-24}

As is well known, the trace amount Yb^{2+} in silica glass has an impact on grey loss in silica fiber [34–37]. Unfortunately, in Yb^{3+} doped silica glasses, it is hard to avoid the reduction of trance amount of Yb^{3+} into Yb^{2+} especially by sol-gel method. In present study, co-doping of P^{5+} in YAF glass strongly reduces the concentration of Yb^{2+}. This is witnessed by the apparent color change of core glass under sunlight, as shown in Fig. 2(b). YA and YAF glasses yield light yellow color due to the strong absorption of Yb^{2+}. On contrary, YAFP1 glass is colorless hinting the low concentration of Yb^{2+}, which favors for the high-power fiber lasers. Figure 3(e) shows absorption spectra of YA, YAF and YAFP1 glasses in UV-visible region. YA glass shows a broad absorption band from ~300 to 450 nm, which is attributed to the 4f → 5d transition of Yb^{2+}. J. Kirchhof [35] proposed an estimation of the quantitative amount of Yb^{2+} by OH formation and derived an absorption coefficient of about 5×10^2 cm^{-1} $(mol\%Yb^{2+})^{-1}$. Based on the absorption coefficient of Yb^{2+} at 330 nm, we calculated the contents of Yb^{2+} in our samples. The contents of Yb^{2+} in YA, YAF and YAFP samples are about 22 ppm, 31 ppm and 12 ppm (molar fraction), respectively. Co-doping of F^- in YA glass can reinforce the absorption intensity of Yb^{2+}. Consequently, YA and YAF glasses yields light yellow color under sunlight. On the contrary, the co-doping of F^-/P^{5+} (YAFP1) in YA glass strongly decreases the absorption intensity of Yb^{2+}. This may be ascribed to the oxidation of P^{5+} addition. The weak absorption of Yb^{2+} in YAFP1 glass endows its colorless nature under sunlight. This is fully consistent with the emission spectra [Fig. 3(f)], which will be discussed later. The low concentration of Yb^{2+} in YAFP glass favors for scaling output power of LMA PCF.

With excitation at 330 nm, YA, YAF and YAFP1 glasses show a bright bluish green emission, as illustrated in inset of Fig. 3(f). The corresponding emission spectra span almost

Optics EXPRESS

the whole visible spectrum from 400 to 700 nm with a maximum at ~520 nm and full width at half maximum of ~150 nm, arising from the 5d → 4f transition of Yb^{2+}. Fully consistent with absorption spectra [Fig. 3(e)], the co-doping F^- slightly increase the emission intensity of Yb^{2+}, whereas the co-doping of F^-/P^{5+} in YA glass strongly decrease the emission intensity of Yb^{2+}, which further proofs the effective oxidation of Yb^{2+} by co-doping of F^-/P^{5+} in YA glass.

3.3 Laser performance of LMA PCF

By using YAFP2 glass rod (⌀5 mm × 90 mm) as core, a LMA PCF fiber was successfully prepared by stock and drawing method. Its cross section is illustrated in Fig. 4(a). The diameters of core, inner cladding and outer cladding are 50 μm, 260 μm and 450 μm, respectively. The diameter of the air holes is ~2.5 μm, while the pitch is ~20 μm. A 6.5 m long PCF was employed for the pulse laser amplification experiment. Figure 4(b) schematically shows the laser amplification experiment setup. A seed source at 1030 nm with a repetition rate of 49.8 MHz and pulse duration of 21 ps was used in this system. The pump source was a 976-nm laser diode (pump 2). Figure 4(c) shows the typical output laser spectrum under irradiation of a 150 W pump power and Fig. 4(d) shows the measured average output power as a function of incident pump power. A maximum amplified output power up to 97 W (corresponding to the pulse energy of 2 μJ) was achieved. We did not observe obvious signal decrease with 30 minutes under irradiation of 150 W pump power in the test process. The further enhancement of the output power is limited by the upper limit of the pump power. The light-light efficiency (with respect to the incident pump power) is calculated to be 54%.

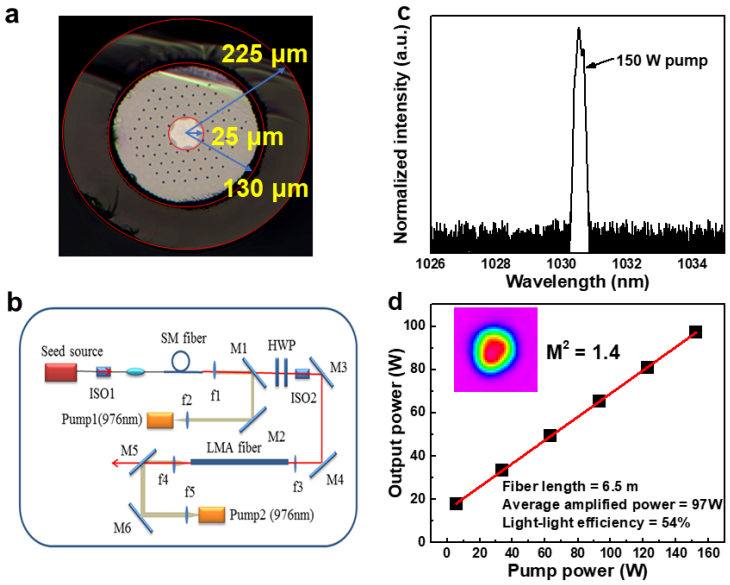

Fig. 4. (a) Micrograph of LMA PCF cross section. (b) Experimental setup of a master oscillator power amplifier system. (c) The output laser spectrum with pumping power of 150 W. (d) Measured amplified output power as a function of pump power. Inset: laser beam profile in the far field.

The inset of Fig. 4(d) shows the laser beam profile in the far field (corresponding to the output power of 97 W). The quasi-single-mode laser operation is obtained and the laser beam quality factor M^2 is determined to be 1.4, which favors for scaling output power of LMA PCF amplifiers. The low NA of YAFP2 core glass (0.027) is responsible for realization of quasi-single-mode laser. We believe that the higher output power can be achieved by further optimization of the doping combination of $Yb^{3+}/Al^{3+}/F^-/P^{5+}$ in silica-core glass, the

Optics EXPRESS

fabrication techniques of silica-core glass and PCF drawing, and applying higher pump power, which will be our future work.

4. Conclusions

In this work, $Yb^{3+}/Al^{3+}/P^{5+}/F^{-}$-co-doped silica glass was prepared by a modified sol-gel method combined with high-temperature sintering, and its optical and spectroscopic properties were systematically studied. Co-doping by F^{-} and F^{-}/P^{5+} at present doping levels maintains or even improves the excellent spectroscopic properties of Yb^{3+} in YA glass. The light shifts of the peak positions in absorption and emission spectra hint the mild modification of local environment around Yb^{3+} by co-doping of F^{-} or F^{-}/P^{5+} in YA glasses. Also, the co-doping of F^{-}/P^{5+} in YA glass strongly decreases the absorption intensity of Yb^{2+} in our samples.

A large-size (⌀5 × 90 mm) $Yb^{3+}/Al^{3+}/P^{5+}/F^{-}$-co-doped silica core glass rod with average refractive index 2.6×10^{-4} above that of pure silica glass was prepared. The corresponding refractive index fluctuations in radial and axial directions are ~2×10^{-4}. To the best our knowledge, this is first-time report of large-size $Yb^{3+}/Al^{3+}/P^{5+}/F^{-}$-co-doped silica core glass rod with such a low refractive index and good optical homogeneity by non-MCVD method. Using this core-glass rod, a LMA PCF with a core diameter of 50 μm was prepared. An average amplified power of 97 W and average light-light efficiency of 54% from a 6.5 m length fiber were achieved. The laser beam resulted in quasi-single-mode transmission with M^2 of 1.4. This $Yb^{3+}/Al^{3+}/P^{5+}/F^{-}$-co-doped silica glass prepared by sol-gel method combined with high temperature sintering is suitable to fabricate lower NA LMA Yb^{3+}-doped silica fibers for high-power lasers.

Funding

National Natural Science Foundation of China (Grant No. 61505232 and No. 61405215); Youth Innovation Promotion Association of the Chinese Academy of Sciences; National High Technology Research and Development Program of China (2016YFB0402201).